Application of new aptasensor modified with nanocomposite for selective estradiol valerate determination in pharmaceutical and real biological samples

Amina Touati, Mohamed Braiek, Messaoud Benounis, Nicole Jaffrezic-Renault

Application of new aptasensor modified with nanocomposite for selective estradiol valerate determination in pharmaceutical and real biological samples

Amina Touati[1] ● Mohamed Braiek[2] ● Messaoud Benounis[1] ● Nicole Jaffrezic-Renault[2]

Received: ……/Accepted …

Abstract

In this study we developed a highly sensitive aptasensor based on polyaniline electro-polymerization, new nanomembrane composite, and aptamer (PANI-MWCNT@Chs-APT) for the electrochemical detection of estradiol valerate in real samples. The high sensitivity and selectivity of the aptasensor were demonstrated by evaluating its response to some potential interference having structural similarities. The selectivity of this aptasensor showed high selectivity for estradiol valerate among other interfering hormones. Electrochemical impedance spectroscopy combined with the standard added method used to characterize the modified gold electrodes as well as for the detection of estradiol valerate both in pharmaceutical and in women's blood. It showed that the response of the aptasensor rose with increasing estradiol valerate concentration, which highlighted the good sensitivity of the

aptasensor to estradiol valerate with a very low limit of detection of 0.56 fM. This was very promising for rapid analysis of estradiol valerate detection in pharmaceutical and biological samples.

Graphical abstract

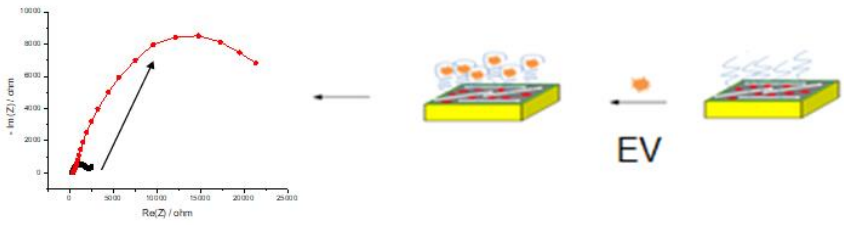

Keywords Biosensor ● Aptamer ● Carbon Nanotubes ● Chitosan ● Blood samples

✉ Amina Touati
touati.amina@univ-khenchela.dz
[1] Laboratory of Sensors, Instrumentations and Process (LCIP), Institute of Science and Technology, Abbes Laghrour University, Khenchela, 40000, Algeria
[2] Laboratory of Analytical Sciences, University Claude Bernard, Lyon 143, Boulevard of 11 November 1918, Villeurbanne Cedex, France, 69622

Introduction

Oestradiol (E2) is a major female sex hormone. According to Ettawfik Medical Analysis Laboratory, normal levels of E2 for menstruating women range from 18 to 147 pg/cm^3. For postmenopausal, E2 levels is lower than 10 pg/cm^3. Lower levels of E2 in the body may suggest late puberty, hypopituitarism, hypogonadism, Turner syndrome, and menopause. Whereas E2 levels that are higher than normal may suggest tumors in the ovaries, early puberty, and scarring of the liver. Estradiol valerate (EV, Fig. 1) is essentially the ester of E2 characterized by the presence of a substitution radical at carbon 17 such as the radical. Following absorption in the body, the ester was cleaved, and the natural estrogen (E2) resulted [1]. EV is very significant in clinical medicine and could be used to treat menopause syndrome and prostate cancer. This hormone can be utilized together with a progestogen for the inhibition of ovulation [2]. As a result, many clinical studies have reported the use of different detection techniques such as HPLC [3, 4] and LC-MS/MS [5], CG/MS [6, 7] for the quantification of EV in diverse samples. Thus, given the high cost, time requirements, and expensive instruments. The development of rapid, simple, selective, less expensive, sensitive, and specific analytical methods for the detection of EV is of great importance.

Several biosensors have been developed for electrochemical detection of natural E2 [8-12] and, to our knowledge; few research articles have been published for synthetic E2 detection [13-15]. Mofidi et al. [13] have developed an electrochemical sensor for EV in blood samples; a carbon paste electrode was modified with terbium carbonate nanoparticles for EV determination. The method showed a limit detection of 0.1 ng/cm^3 with a linear range of 13×10^2 - 10×10^3 ng/cm^3. In this study, EV was extracted from the blood sample with a recovery percentage of 67%. Various electrochemical methods are based on aptamer-based biosensors for the detection of E2 in real samples [16-20].

Recently, many aptasensor based on nanomaterial electrochemical electrode-modifying has received a huge amount of attention due to their inherent advantages such as high specific surface area and excellent electrical performance of nanomaterials such as simplicity, high sensitivity, low cost, and high stability [21-24]. Hlavata et al. [25] have developed an electrochemical biosensor based on nanomaterials, by combining the benefits of chitosan and carboxylate single-walled carbon nanotubes for evaluation of damage to DNA induced by UV-C radiation. They were studied the role of these nanomaterials (with and without carbon nanotube) for the performance of biosensors and they deduced that the utilization of carbon nanotubes increasing the electro-conducting properties of the

biosensor. In another report, Nameghi et al. [26] have proposed a simple electrochemical aptasensor for E2 in a blood sample. In this sensor platform, a split DNA aptamer was applied as recognizing agents with E2. The aptasensor was indicated a wide linear range with detection limits of 0.7 pM and 0.5 pM for E2 in milk samples and tap water, respectively.

In this study, we developed a highly sensitive aptasensor based on PANI-MWCNT@Chs-APT composite for the electrochemical detection of estradiol valerate (EV) in real samples. The elaboration of the aptasensor involves a three-step modification process. First, we carried out the electrochemical polymerization of aniline (polyaniline (PANI)) on the gold electrode (AuE). Secondly, the MWCNT@Chs was prepared and dropped to the surface of electropolymerized gold to form MWCNT@Chs/PANI/AuE. This new membrane has been developed by Ying Ou et al.; the MWCNTs were functionalized by the polyelectrolyte Chs, via a noncovalent surface deposition method [27]. Finally, the free carboxyl groups on the MWCNT@Chs/PANI/AuE surface were conjugated with the NH_2–Aptamer to afford an aptasensor APT/MWCNT@Chs/PANI/AuE interface. Electrochemical impedance spectroscopy (EIS) was used for gold electrodes (AuE) characterization and it combined with a standard added method to evaluate the performance of

aptasensor developed. This method has seen a huge boost in popularity in recent times due to its extraordinary sensitivity.

< Figure 1 >

Results and Discussion

Characterization of the aptasensor surface

EIS could be the effective method to study the interface characteristics of modified electrodes. Figure 2 showed the Nyquist plots comparison of different modified electrodes of AuE, AuE/PANI, AuE/PANI/ MWCNTs@Chs, and AuE/PANI/ MWCNTs@Chs/APT. The EIS of the bare AuE displays quite small semicircle diameters, implying a low resistance charge transfer (R_{CT}) to the redox probe in $[Fe(CN)_6]^{3-}$/ $[Fe(CN)_6]^{4-}$ electrolyte solution. While the value of R_{CT} increases after the PANI was modified on the AuE electrode, this might be ascribed to the less-conductive polymers. However, the R_{CT} of PANI/MWNTs@Chs was decreased gradually because PANI could promote electron transfer. After aptamer immobilized on AuE/PANI/MWNTs@Chs, the R_{CT} rose significantly because the formed aptamer layer prevented the electron transfer. EIS data are commonly analyzed by fitting a Randles equivalent circuit model (Fig. 2 inset). This circuit was adapted by replacing the ideal

capacitor with a constant phase element (CPE). The presence of the diffusion limitations at low frequencies must also be presented in the circuit and was represented by a Warburg element (Z_W). The obtained semi-circle indicates that multiple processes with different time constants occurred. The high-frequency values resulted from processes in the electrolyte or electrode bulk (conductivity), whereas the low-frequency values resulted from processes at the electrode-electrolyte interface (double layer, charge transfer) or the electrode surface (mass transport, adsorption, electrochemical reactions) [28].

< Figure 2 >

Optimization of aptamer concentration

The optimization of aptamer concentration is an essential step that affects the performance of the developed aptasensor. Therefore, three different concentrations of aptamer (0.40, 1.21, and 2.02 mM) were tested within the range of 4×10^{-16} to 4×10^{-10} mg/cm^3 of EV using the EIS device. Figure 3 shows the variation of R_{ct}^{f} as function of the EV concentrations for the aptamer concentrations. The calibration curves (Fig. 3) show a comparison between the relative slopes of three aptasensors; as it can be observed, when

using the aptamer concentration (2.02 mM) the aptasensor presents a good linear response towards the different [EV], with high sensitivity.

< Figure 3 >

Detection of EV in pharmaceutical samples

To evaluate the effectiveness of aptasensor developed (APT/MWCNT@Chs/PANI/AuE) to quantify EV in pharmaceutical samples. Two pills of (progenovat®2mg) were dissolved in 25 cm^3 of PBS (5 mM pH 7.4) and sonicated for 10 min. Various EV concentrations in the range of 4×10^{-16} to 4×10^{-9} mg/cm^3 were prepared using PBS. EIS measurements were carried out to detect EV in these solutions at a frequency ranging from 100 kHz to 100 mHz. The aptasensor was incubated with different concentrations of EV for 30 min at room temperature, and then the response of the aptasensor was determined (Fig. 4(A)).

The normalized data was presented as the change to film resistance (R_{ct}^{f}) as a function of EV concentrations is plotted in Fig. 4(B). The R_{ct}^{f} was calculated according to the equation:

$$R_{ct}^{f} = \frac{R_{ct}^{C} - R_{ct}^{C=0}}{R_{ct}^{C=0}} \quad (1)$$

where R_{ct}^{C} and $R_{ct}^{C=0}$ are the values of the charge transfer resistance before and after the incubation in EV concentrations.

Figure 4(A) showed that the Nyquist plot of the interface aptasesor at different concentrations of EV. The R_{CT} values were found to rise (from 12 to 51.5 kΩ) with increasing concentration of EV from 4×10^{-16} to 4×10^{-9} mg/cm³. This was due to the increased complexation by adsorption of EV onto the aptasensor interface; it was directly related to the good sensitivity of the modified electrode to EV.

It could be seen in the calibration plot (Fig. 4(B)), a linear dependence between the R_{ct}^{f} values and the logarithmic values of EV concentration. The calibration curve equation was obtained by Origin 9.1 version via plotting and analyzing:

$$R_{ct}^{f}/\Omega = 0.46 \text{ Log } ([EV] /\text{mg cm}^{-3}) + 7.41 \quad (2)$$

The aptasensor had a linear response in the range of EV concentrations between 4×10^{-16} to 4×10^{-9} mg/cm³ with a good correlation coefficient of about 0.996 and a high sensitivity of 0.46 Ω per EV concentration decade. While the limit of detection was calculated to be 0.56 fM from the calibration curve by three times the standard deviation of the average value of the blank without adding the EV standard solution (n=5), divided by the sensitivity. This LOD was lower than those reported in the references [23, 31, 32, 34] and it was in good agreement with those attained by other sensors [29, 30,

36] (Table 1). This lower limit detection was attributed by Ke et al. [30]; after estradiol reacts with aptamer, the interfacial electron transfer resistance was enlarged on the electrode surface thus the reason for the rise of impedance. These results indicated that the prepared aptasensor could be safely used for the determination of [EV] in the pharmaceutical samples.

In this work, the role of carbon nanotube for aptamer immobilization was investigated. The aptamer was directly fixed on the PANI layer, without nanotubes (Fig. 4(B)). These results showed that the performance of APT/PANI/AuE aptasensor could be significantly degraded with the absence of MWCNTS.

< Figure 4 >

Study of interferences

The developed aptasensor was evaluated for the selectivity studies by comparing it with some interference having structural similarities with EV such as DCI and P4, all at various concentrations ranging from 4×10^{-16} to 4×10^{-9} mg/cm³. Using 5 mM PBS electrolyte at pH 7.4. The specificity of the APT/MWCNT@Chs/PANI/AuE aptasensor for different interfering elements is shown in Fig. 5. From these results, we could deduce that this aptasensor had a high selectivity towards EV and E2, with a much lower

response to all other hormones tested. This indicates that we can use this aptasensor to detect the synthetic estradiol in real samples.

< Figure 5 >

Detection of EV in real biological samples

The developed aptasensor was used to estimate EV concentrations in the blood sample by the standard addition method combined with EIS. A blood sample (on the third day of menstruation) was centrifuged for 10 min. 1 cm^3 of serum obtained was diluted in 24 cm^3 of PBS pH 7.4. Different concentrations of EV were prepared in PBS from 4×10^{-16} to 4×10^{-10} mg/cm^3. 1 cm^3 of each EV concentration was added to each of the seven volumetric flasks of 2 cm^3. To obtain the final volume of 2 cm^3, 1 cm^3 of the serum sample was added to each of the seven volumetric flasks. The Nyquist plot of the platform aptasensor at different concentrations of EV in serum samples was shown in Fig. 6(A). It could be seen from the plot that the diameter of the curve increased with the growing concentration of EV, indicating a decrease in the conductance of the samples. The values of R_{CT} rose with the increasing concentration of EV, which was responsible for the decrease in the double layer capacitance appearing at the electrode-electrolyte interface. The calibration curve equation was obtained:

$$R_{ct}^{f}/\Omega = 6.473 \text{ Log } ([\text{EV}] /\text{mg cm}^{-3}) + 79.21 \quad (3)$$

The concentration of EV in the unknown serum sample obtained by the standard addition method was 43.15 pg/cm^3.

The concentration of this plasma sample was also tested using the immuno-electrochimiluminescene ”ECLIA” (Cobas, Roche). The result obtained was 41.25 pg/cm^3. Both results were nearly the same with a recovery = 95 %. However, this result was in line with the estradiol levels determined in the blood samples of healthy women during menstruation range from (18 to 147 pg/cm^3). These results indicated that the developed aptasensor could be applied in real pharmaceutical applications.

< Figure 6 >

< Table 1 >

Conclusion

In this work, a new sensitive and selective aptasensor was developed and successfully applied to determine EV in pharmaceutical and real female blood samples. We showed that the APT/MWCNT@Chs/PANI/AuE aptasensor exhibited excellent performances with high sensitivity and selectivity. A good linear relationship was also obtained between the R_{CT} values and the logarithmic values of EV concentration with a lower LOD of

about 0.56 fM both in pharmaceutical and women's blood. Therefore, this work could provide a potential tool for the rapid detection of EV in real samples.

Experimental

(Progynova®) was employed from Delpharm Lille S.A.S (France). Progesterone (P4) was obtained from Laboratoires BESINS International (France). Methylprednisolone (DCI) was produced from Valdepharm (France). 17β-Estradiol (E2), multi-walled carbon nanotube (MWNTs), chitosan (Chs, *75%* deacetylated), glutaraldehyde (GA) (grade II, 25% aqueous solution), potassium ferricyanide ($K_3[Fe(CN)_6]$), potassium ferrocyanide ($K_4[Fe(CN)_6]$), ammonia, phosphate buffer solution (pH 7.4), nitric acid, hydrogen peroxide solution, acetone, sulfuric acid, hydrogen peroxide, and ethanol were obtained from Sigma-Aldrich (France). Aniline and acetic acid were obtained from VWR International S.A.S (France). *N*-Hydroxysuccinimide (NHS) and *N*-(3-dimethylaminopropyl)-*N′*-ethylcarbodiimide (EDC) were received from Shanghai Yuanye BioTechnology Co., Ltd. (China). Gold substrates were provided by the French RENATECH network (LAAS, CNRS Toulouse). The single-strand DNA Aptaanti-oestradiol was chosen according to the prior reported literature [37]; then, was obtained from Eurogentec, the sequence of the 76-

mersized amino-modified aptamer as follows: (5'-amino-modified): 5'-GCT-TCC-AGC-TTA-TTG-AAT-TAC-ACG-CAG-AGG-GTA-GCG-GCT-CTG-CGC-ATT-CAA-TTG-CTG-CGC-GCT-GAA-GCG-CGG-AAGC-3'). After Jenison et al and Kato et al.; the dissociation constants for (10ssDNA) aptamers were in the range of (0.1-3 μM) [38, 39]. The stock (EV, P4, and DCI) samples (4±0.04 mg/cm³) were obtained by dissolving in PBS buffer (5 mM, pH 7.4) and stored at 4 ℃ for experiments.

All the electrochemical measurements were carried out in a Faraday box at room temperature using an SP-300 Potentiostat/Galvanostat/FRA (BioLogic Science Instruments SAS, France) controlled by EC-Lab software with a three-electrode cell system, which consists of a gold electrode (AuE: 0.78 mm^2), a platinum wire (Pt), and an electrode calomel (saturated KCl) used as the working, counter, and reference electrodes, respectively.

Cyclic voltammetry (CV) was used for electrochemical polymerization of aniline on the surface of gold electrodes within potential scan limits of -0.2 to 1.4 V at a potential scan rate of 100 mV s^{-1}.

The electrochemical impedance spectroscopy (EIS) measurements combined with the standard added method were used to evaluate the performance of the aptasensor developed. Furthermore, the EIS was analyzed over a frequency range from 100 mHz to 100 kHz at a potential of 128 mV and an amplitude of 10 mV. The obtained data EIS were fitted by

Randles equivalent circuit model. The validation of this model is obtained by comparing the experimental data to the theoretical EIS model using EC-Lab software with the Randomize + Simplex method. This device was then used to detect EV, both in pharmaceutical and blood women, these samples were diluted in PBS at pH 7.4 within the range 4.0×10^{-16} to 4.0×10^{-9} mg/cm³. The impedance response was recorded by successive incubations for 30 min of interface aptasensor in real samples containing different concentrations of EV.

Elaboration of the aptasensor (APT/MWCNTs@Chs/PANI/AuE)

Electropolymerization of aniline on gold electrode

Before modification, the gold electrodes were cleaned with acetone and sonicated in ultrapure water. Then, dipped into a piranha solution (3:1 mixture of concentrated H_2SO_4 with H_2O_2) for 4 min and washed with ethanol and ultrapure water. Next, the electrodes were electrochemically cleaned in 0.5 M H_2SO_4 in the potential scanning between -0.5 V and 1.5 V for 5 min, followed by washing them with ultrapure water and drying under nitrogen. After that, the electrochemical polymerization of AuE electrode had been performed in 0.5 M sulfuric acid solution containing 0.1 M of aniline by potential cycling within the potential scan limits of -0.2 to 1.4 V

for 30 cycles at a potential scan rate of 100 mV s^{-1} (Fig. 7). This technology of functionalization was recently detailed in various papers [40-43].

< Figure 7 >

Preparation of nanomembrane (Chs@ MWCNTs)

First, the pristine MWCNTs (200 mg) were oxidized by 80 cm^3 of a concentrated H_2SO_4 (98 %) and HNO_3 (65 %) solution mixed at a volume ratio of 3:1 under ultrasonic oscillation at 70 °C for 3 h to obtain carboxylated HOOC-MWCNTs [44]. The resulting HOOC-MWCNTs were rinsed several times with double distilled water until the pH reached 7.0 and then dried in a vacuum freeze dryer. This process was for the open of the ends of long tubes and the introduction of carboxyl groups to the surface [45]. Secondly, the Chs@MWCNTs were prepared by the process of Ou et al. (2018) using a noncovalent surface-deposition and cross-linking method. Briefly, 100 mg of MWCNTs was dispersed in a Chs solution (0.1 g Chs in 100 cm^3 1 vol. % acetic acid solution). Diluted ammonia solution was added dropwise to the dispersion to adjust pH = 9. Subsequently, the obtained suspension was heated to 60 °C and 0.02 g of GA was added to cross-link the surface deposited Chs for 1 h. Finally, the Chs@MWCNTs products were collected by centrifugation and then washed with dilute acetic acid to

remove the adsorbed and uncross-linked Chs [27]. Then, 5 mm^3 of Chs@MWCNTs dispersion was dropped by drop added to the surface of the electropolymerized gold electrode and dried at room temperature for 5 h.

Immobilization of aptamer

Before the aptamer immobilization, NHS/EDC technique was used to activate the –COOH groups of the aptamer. Briefly, 50 mm^3 of aptamer (4.04 mM) were mixed with 50 mm^3 of the PBS solution containing (0.1 M NHS/0.4 M EDC). 6 mm^3 of the activated aptamer was then dropped on the MWCNT@Chs/PANI/AuE electrode and maintained for 24 h at room temperature for immobilization. Afterward, the remained active carboxylic acid groups were deactivated by incubating them in the ethanolamine solution (1% in PBS) at room temperature for 20 min. This stage is very important to prevent nonspecific bonding at the detection step [46]. The whole construction procedure of the modified aptasensor was displayed in Fig. 8 and the resulting electrode is called APT/MWCNT@Chs/PANI/AuE electrode.

< Figure 8 >

EIS was used for modified electrodes (bare AuE, PANI/AuE, MWCNTs@Chs/PANI/AuE and APT/MWCNT@Chs/PANI/AuE) characterization using 5 mM of $[Fe(CN)_6]^{3-}$/ $[Fe(CN)_6]^{4-}$ (Fig. 2).

References

1. Robert HG, Palmer R, Boury-Heyler C (1974) Précis de gynécologie. Masson et Cie, p 323
2. Ping Duan J, Qin Chen H, Nan Chen G, Li Chen M, Ping Wu X (1999) Analyst 124:1651
3. Kwok KY, Choi TL, Kwok WH, Wong JK, Wan TS (2017) J Chromatogr A 1493:76
4. Kaabia Z, Dervilly-Pinel G, Hanganu F, Cesbron N, Bichon E, Popot M, Bonnaire Y, Le Bizec B (2013) J Chromatogr A 1284:126
5. Ferreira MS, Arruda AM, Pepi GT, Martho AC, Maximiano PM, Ricci LS, Riccio MF, Noboli AC, Júnior PS (2017) J Chromatogr B 1064:109
6. Yilmaz B (2010) Anal Sci 26:391
7. Zhou Y, Zha J, Xu Y, Lei B, Wang Z (2012) Environ Monit Assess 184:1719
8. Ochiai LM, Agustini D, Figueiredo-Filho LC, Banks CE, Marcolino-Junior LH, Bergamini MF (2017) Sens Actuators B Chem 241:978

9. Lahcen AA, Baleg AA, Baker P, Iwuoha E, Amine A (2017) Sens Actuators B Chem 241:698
10. Li J, Jiang J, Zhao D, Xu Z, Liu M, Deng P, Liu X, Yang C, Qian D, Xie H (2018) J Alloys Compd 769:566
11. Wang Y, Luo J, Liu J, Li X, Kong Z, Jin H, Cai X (2018) Biosens Bioelectron 107:47
12. Wang A, Ding Y, Li L, Duan D, Mei Q, Zhuang Q, Cui S, He X (2019) Talanta 192:478
13. Mofidi Z, Norouzi P, Larijani B, Seidi S, Ganjali MR, Morshedi M (2018) J Electroanal Chem 813:83
14. Triviño JJ, Gómez M, Valenzuela J, Vera A, Arancibia V (2019) Sens Actuators B Chem 297:126728
15. Bergamin B, Pupin RR, Wong A, Sotomayor MD (2019) J Braz Chem Soc 30:2344
16. Liu M, Ke H, Sun C, Wang G, Wang Y, Zhao G (2019) Talanta 194:266
17. Raj M, Goyal RN (2019) Sens Actuators B Chem 284:759
18. Zhang G, Li T, Zhang J, Chen A (2018) Sens Actuators B Chem 273:1648
19. Antoniazzi C, de Lima CA, Marangoni R, Spinelli A, de Castro EG (2018) J Solid State Electrochem 22:1373

20. Eletxigerra U, Martinez-Perdiguero J, Merino S, Barderas R, Montiel VR-V, Villalonga R, Pingarrón J, Campuzano S (2016) Sens Biosensing Res 7:71
21. Huang K-J, Liu Y-J, Zhang J-Z, Cao J-T, Liu Y-M (2015) Biosens Bioelectron 67:184
22. Nezami A, Nosrati R, Golichenari B, Rezaee R, Chatzidakis GI, Tsatsakis AM, Karimi G (2017) Trends Anal Chem 94:95
23. Huang K-J, Liu Y-J, Zhang J-Z (2015) Microchim Acta 182:409
24. Hui Y, Wang B, Ren R, Zhao A, Zhang F, Song S, He Y (2020) Food Control 109:106902
25. Hlavata L, Benikova K, Vyskocil V, Labuda J (2012) Electrochim Acta 71:134
26. Nameghi M, Danesh N, Ramezani M, Alibolandi M, Abnous K, Taghdisi S (2019) Anal Chim Acta 1065:107
27. Ou Y, Tsen WC, Gong C, Wang J, Liu H, Zheng G, Qin C, Wen S (2018) Polym Adv Technol 29:612
28. Pilehvar S, Dierckx T, Blust R, Breugelmans T, De Wael K (2014) Sensors 14:12059
29. Rather JA, Khudaish EA, Kannan P (2018) Analyst 143:1835
30. Ke H, Liu M, Zhuang L, Li Z, Fan L, Zhao G (2014) Electrochim Acta 137:146

31. Jiang Y, Colazo MG, Serpe MJ (2018) Anal Bioanal Chem 410:4397
32. Qi X, Hu H, Yang Y, Piao Y (2018) Analyst 143:4163
33. Kumbhat S, Gehlot R, Sharma K, Singh U, Joshi V (2019) J Pharm Biomed Anal 163:211
34. Cao N, Zeng P, Zhao F, Zeng B (2018) Electrochim Acta 291:18
35. Pu H, Xie X, Sun D-W, Wei Q, Jiang Y (2019) Talanta 195:419
36. Dharuman V, Hahn JH, Jayakumar K, Teng W (2013) Electrochim Acta 114:590
37. Kim YS, Jung HS, Matsuura T, Lee HY, Kawai T, Gu MB (2007) Biosens Bioelectron 22:2525
38. Jenison RD, Gill SC, Pardi A, Polisky B (1994) Science 263:1425
39. Kato T, Takemura T, Yano K, Ikebukuro K, Karube I (2000) Biochim Biophys Acta Gene Struct Expr 1493:12
40. Gandara M, Gonçalves ES (2020) Prog Org Coat 138:105399
41. Mažeikienė R, Niaura G, Malinauskas A (2018) J Electroanal Chem 808:228
42. Deshmukh MA, Celiesiute R, Ramanaviciene A, Shirsat MD, Ramanavicius A (2018) Electrochim Acta 259:930
43. Parvin MH, Arjomandi J, Lee JY (2018) Catal Commun 110:59

44. Nie Y (2012) Surface silanization of carbon nanofibers and nanotubes for altering the properties of epoxy composites. https://nbn-resolving.org/urn:nbn:de:gbv:ilm1-2012000133
45. He B, Du G (2018) Anal Bioanal Chem 410:2901
46. Bellagambi FG, Baraket A, Longo A, Vatteroni M, Zine N, Bausells J, Fuoco R, Di Francesco F, Salvo P, Karanasiou GS (2017) Sens Actuators B Chem 251:1026

Figure Captions

Fig. 1 Chemical structure of oestradiol (E2), estradiol valerate (EV), methylprednisolone (DCI), and progesterone (P4)

Fig. 2 Nyquist plots of 5 mM $[Fe(CN)6]^{3-}$/$[Fe(CN)6]^{4-}$) obtained at (a) bare AuE, (b) PANI/AuE, (c) MWCNTs@Chs/PANI/AuE, (d) APT/MWCNTs@Chs/PANI/AuE modified electrodes. The frequency range from100 mHz to 100 kHz. The inset shows the equivalent circuit used to model impedance data

Fig. 3 Optimization of EV-aptamer concentration; (▲) 0.40 mM, (●) 1.21 mM, and (■) 2.02mM of aptamer

Fig. 4 (A) Nyquist plots of APT/MWCNT@Chs/PANI/AuE aptasensor at various concentrations of EV in 5 mM PBS (pH 7.4). (B) Calibration curve of APT/MWCNT@Chs/PANI/AuE and APT/PANI/AuE aptasensors at various concentrations of EV in 5mM PBS (pH 7.4) (n=3)

Fig. 5 Specificity of the aptasensor for the detection of (a) EV by comparing it with (b) E2, (c) DCI, and (d) P4. All at various concentrations range from 4×10^{-16} to 4×10^{-9} mg/cm³ in 5 mM PBS at pH 7.4 (n=3)

Fig. 6 (A) Nyquist impedance plots (Zr vs Zi) obtained from the standard addition method performed on a serum blood sample at 5 mM of PBS pH 7.4 solution. (B) Calibration curve used to determine the concentration of EV in the unknown Serum sample by the standard addition method (n=3), $R^2 = 0.996$

Fig. 7 Cyclic voltammograms of electrochemical polymerization of aniline on the gold electrode from the aqueous solution of 0.5 M of sulfuric acid containing 0.1 M of aniline, as obtained at a potential scan rate of 100 mV s^{-1} within potential scan limits of -0.2 to 1.4 V

Fig. 8 Construction of the aptasensor APT/MWCNTs@Chs/PANI/AuE interface

Table 1 Performance comparison of APT/MWCNT@Chs/PANI/AuE for the detection of estradiol with other sensors

Estradiol–sensor interfaces	Method	Linearity range /M	LOD /M	Ref.
6-Mercapto-1-hexanol, graphene, DNase I enzyme	DVP	0.07×10^{-12} - 10×10^{-12}	50×10^{-15}	[16]
(CuO/CPE detector)	SWV	60.0×10^{-9} - 800.0×10^{-9}	21.0×10^{-9}	[19]
GOx/APT/AuNPs/CuS/GCE	DVP	$5\ \times10^{-13}$ - 5×10^{-9}	6×10^{-14}	[23]
APT–ERGO/GCE	SWV	1.0×10^{-15} - 0.23×10^{-9}	0.5×10^{-15}	[29]
Hierachical dendritic gold	EIS	10.01×10^{-15}- 1.0×10^{-9}	5.0×10^{-15}	[30]
(pNIPAm)	Sps	3.2×10^{-12} - 711.1×10^{-12}	3.2×10^{-12}	[31]
GN	Fluorescence emission spectra	$0 – 73.42\times10^{-9}$	2.75×10^{-15}	[32]
11-MUA / E2-BSA conjugate on gold sensor chip vs. Ab-E2	SPR	0.036×10^{-12} - 3.6×10^{-12}	3.67×10^{-12}	[33]
Ru@ethyl-SiO_2	ECL	0.037×10^{-12} - 367.12×10^{-12}	1.8×10^{-14}	[34]
DNA-functionalized Au@Ag NPs	SERS	1.0×10^{-13} - 1.0×10^{-9}	2.75×10^{-15}	[35]
Anti-E2/ ITO/ErG/AuNP	CV	1×10^{-3}–0.1×10^{-12}	0.1×10^{-15}	[36]
APT/MWCNT@Chs/PANI	EIS	1.12×10^{-15} - 1.12×10^{-9}	0.56×10^{-15}	This work

APT–ERGO/GCE: electrochemically reduced graphene oxide
DPV: differential pulse voltammetry
CuO/CPE : copper(II) oxide-modified carbon paste electrode
GN: graphite nanoparticle
SPR: surface plasmon resonance
pNIPAm: poly(*N*-isopropylacrylamide) microgel-based etalons
SERS: surface-enhanced raman spectroscopy
Ru@ethyl-SiO_2: $Ru(bpy)_3^{2+}$ Doped vinyl-SiO_2 nanoparticles (Ru@ethyl-SiO_2) and E2 imprinted polypyrrole (MIP)
ECL: electrochemiluminescence
GOx/APT/AuNPs/CuS: glucose oxidase / aptamer / gold nanoparticles / copper sulfide nanosheets
Au@Ag CS NPs: gold-silver core-shell nanoparticles
Anti-E2/ ITO/ErG/AuNP: anti estradiol antibody/indium tin oxide/graphene/gold nanoparticle.

1 *Figure 1*

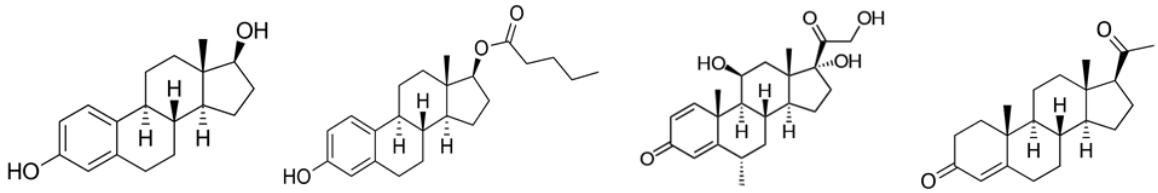

E2 EV DCl P4

2

3

4

5

6

7 *Figure 2*

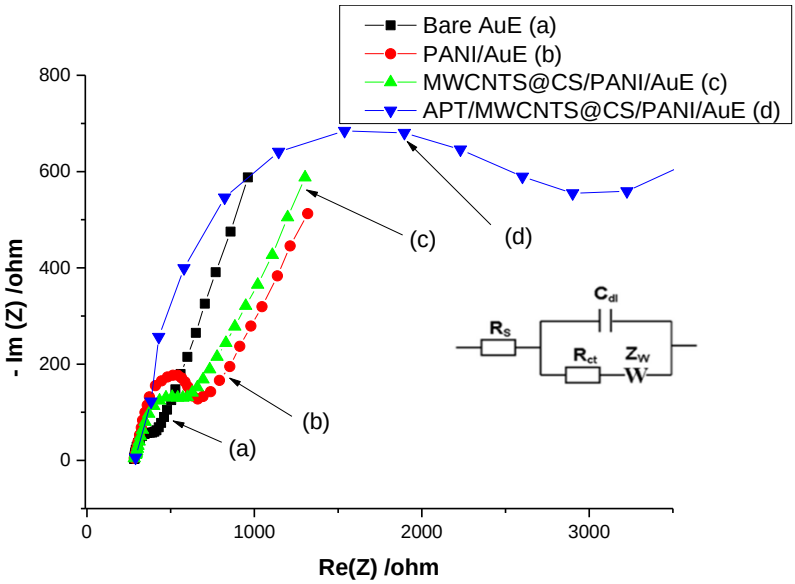

8

9

1 *Figure 3*

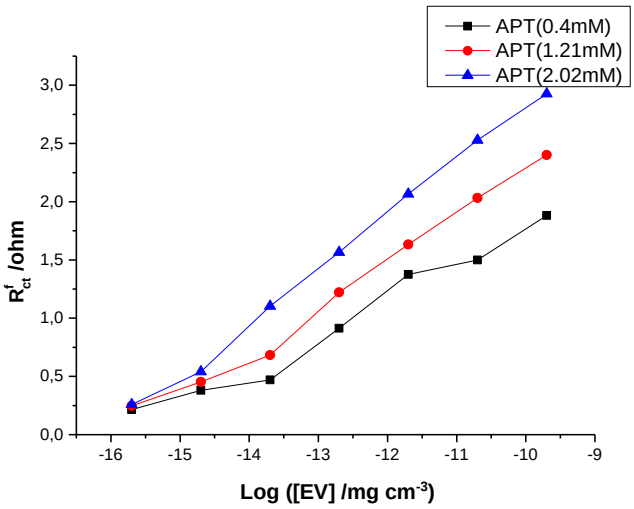

2

3

4

5

6 *Figure 4*

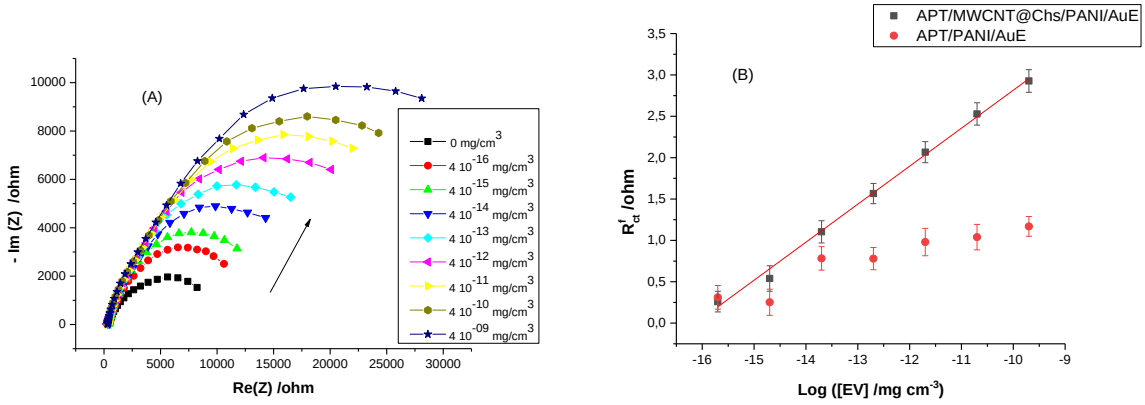

7

8

1 *Figure 5*

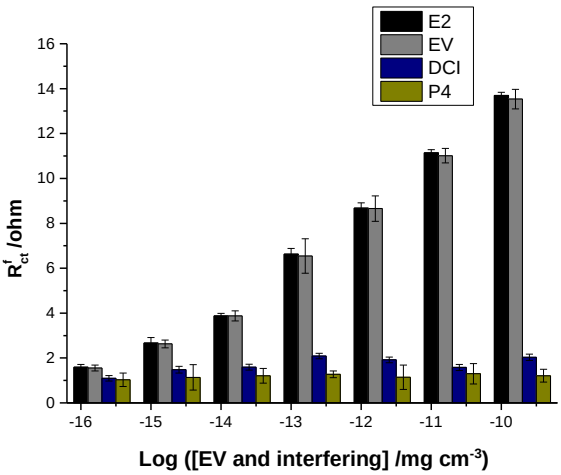

2

3

4

5

6

7 *Figure 6*

8

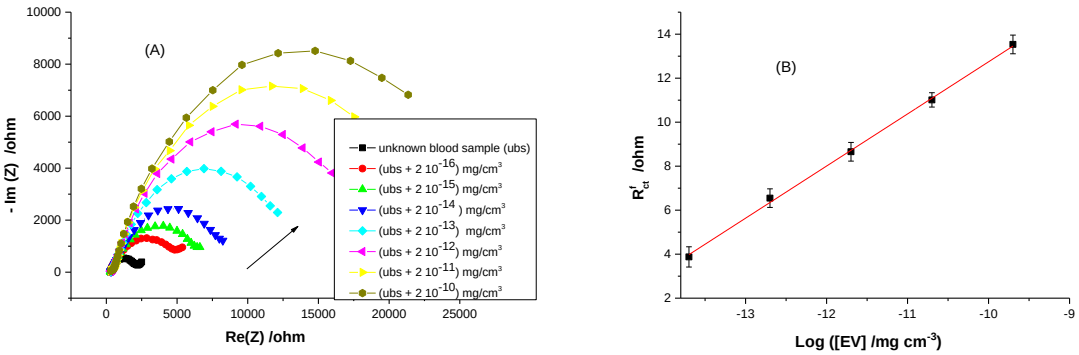

9

10

11

1 *Figure 7*

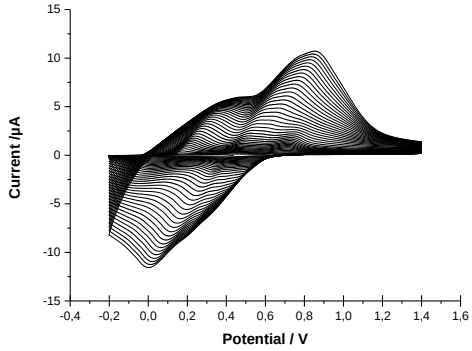

2

3

4 *Figure 8*

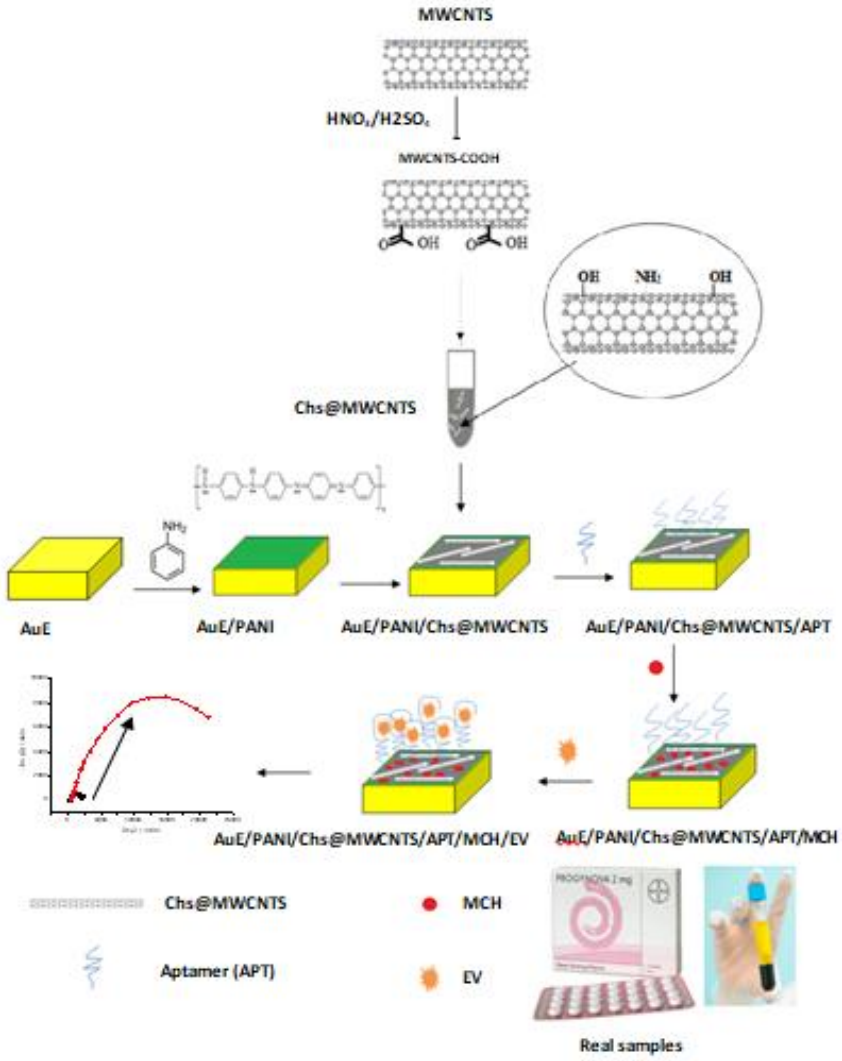

5